VOL. 157, NO. 5 THE AMERICAN NATURALIST MAY 2001

Invasion by Extremes: Population Spread with Variation in Dispersal and Reproduction

James S. Clark,[1,*] Mark Lewis,[2] and Lajos Horvath[2]

1. University Program in Ecology and Department of Biology, Duke University, Durham, North Carolina 27708;
2. Department of Mathematics, University of Utah, Salt Lake City, Utah

Submitted December 27, 1999; Accepted December 15, 2000

ABSTRACT: For populations having dispersal described by fat-tailed kernels (kernels with tails that are not exponentially bounded), asymptotic population spread rates cannot be estimated by traditional models because these models predict continually accelerating (asymptotically infinite) invasion. The impossible predictions come from the fact that the fat-tailed kernels fitted to dispersal data have a quality (nondiscrete individuals and, thus, no moment-generating function) that never applies to data. Real organisms produce finite (and random) numbers of offspring; thus, an empirical moment-generating function can always be determined. Using an alternative method to estimate spread rates in terms of extreme dispersal events, we show that finite estimates can be derived for fat-tailed kernels, and we demonstrate how variable reproduction modifies these rates. Whereas the traditional models define spread rate as the speed of an advancing front describing the expected density of individuals, our alternative definition for spread rate is the expected velocity for the location of the furthest-forward individual in the population. The asymptotic wave speed for a constant net reproductive rate R_0 is approximated as $(1/T)(\pi u R_0/2)^{1/2}$ m yr^{-1}, where T is generation time, and u is a distance parameter (m^2) of Clark et al.'s 2Dt model having shape parameter $p = 1$. From fitted dispersal kernels with fat tails and infinite variance, we derive finite rates of spread and a simple method for numerical estimation. Fitted kernels, with infinite variance, yield distributions of rates of spread that are asymptotically normal and, thus, have finite moments. Variable reproduction can profoundly affect rates of spread. By incorporating the variance in reproduction that results from variable life span, we estimate much lower rates than predicted by the standard approach, which assumes a constant net reproductive rate. Using basic life-history data for trees, we show these estimated rates to be lower than expected from previous analytical models and as interpreted from paleorecords of forest spread at the end of the Pleistocene. Our results suggest reexamination of past rates of spread and the potential for future response to climate change.

Keywords: extreme events, fat-tailed kernels, forest dynamics, Holocene, migration, seed dispersal.

* Corresponding author; e-mail: jimclark@duke.edu.

Am. Nat. 2001. Vol. 157, pp. 537–554. 0003-0147/2001/15705-0006$03.00.

To simplify the problem of tree migration, Skellam (1951) made some assumptions that continue to influence how ecologists analyze invasions. His diffusion model includes a net reproductive rate, R_0, a mean squared dispersal distance, α, which determines the abundance and distribution of offspring, and the average length of a generation, T. For oaks invading Europe at the end of the Pleistocene, Skellam used an example of trees that produce 9,000,000 acorns scattered in a Gaussian pattern, with a generation lag of 50 yr. The rates of spread at the end of the Pleistocene (up to 10^3 m yr^{-1}) required values of α much larger than those inferred from modern dispersal studies. Although a diffusion model did not work well in this instance, successful applications helped popularize these models through the 1990s (Skellam 1951; Lubina and Levin 1988; Andow et al. 1990; van den Bosch et al. 1990; Turchin 1998).

Growing appreciation that a single, constant value of α may not adequately describe dispersal has fostered reconsideration of how variability affects population spread. More complex models, described by dispersal kernels with additional parameters (Kot et al. 1996) or by mixtures (Clark 1998; Clark et al. 1999), can better describe the leptokurtic scatter of offspring, and these models change the predictions of spread. Leptokurtic dispersal kernels describe more short- and long-range dispersers than does a Gaussian kernel having comparable mean and variance. Not only do leptokurtic kernels predict higher spread rates than does a Gaussian kernel with the same variance, but the leptokurtosis in the distribution also produces greater distinction between short- and long-range dispersal events. For example, most acorns fall close to the parent, but jays move some acorns several kilometers (Johnson and Webb 1989). Thus, leptokurtic kernels result in the establishment

of remote subpopulations, which become foci for additional dispersal.

Weinberger (1982) showed that a broad class of models predict that spread rate eventually approaches a constant value, provided that the kernel is exponentially bounded (i.e., has a tail that approaches zero at least as fast as exponential). The value of the constant spread rate depends on the shape of the kernel, more leptokurtic kernels typically yielding a larger value for the constant (Kot et al. 1996). Fat-tailed (exponentially unbounded) kernels result in rapid and patchy expansion that frustrates both field study and analysis (Mollison 1972, 1977). Recently, Kot et al. (1996) used an integrodifference equation population model to approximate the rate of spread when the dispersal kernel is fat tailed. This rate is extremely sensitive to the shape of the tail. In contrast to diffusion, spread accelerates over time. By neglecting the tail when fitting kernels to data, previous studies probably underestimated the potential rate of spread.

Clark (1998) demonstrated that the rate of spread is especially sensitive to the net reproductive rate R_0 when the tail is fat, and the fatter the tail, the greater the sensitivity. The high rates predicted after several generations (for some species, >10 m^2 yr^{-1}) were comparable to paleoevidence for early Holocene spread of forest trees, but stochastic simulations predicted slower spread than the integrodifference equation model.

These new results accommodate some of the variability (i.e., the rare, long-distance events) that Skellam's early analysis ignored, but there are at least two reasons why they may still not provide useful predictions. First, the insights provided by integrodifference equations do not fully translate to data. Although real dispersal may be leptokurtic, unlike some models, data are always bounded. Parametric kernels that best fit data may be fatter than exponential (Taylor 1978; Portnoy and Willson 1993; Turchin 1998) and even lack finite moments (Kot et al. 1996; Clark et al. 1999). But the data themselves are always bounded and have all moments finite. These qualities hold even for data that are simulated from unbounded kernels that lack finite moments. Thus, the unbounded acceleration predicted by parametric models cannot apply to finite offspring. Although Clark (1998) found reasonable agreement with simulation results during early stages of Holocene expansion, the integrodifference equation model with a fat-tailed kernel produces no constant asymptotic wave speed that might be compared to data.

Second, high sensitivity to fecundity suggests that use of mean reproduction (a single value for R_0) may result in poor estimates if reproduction varies. Variability among individuals in fecundity can be extreme, not least due to variable life span. For instance, the importance of a remotely dispersed seed depends on the odds of future success. We might follow Skellam's (1951) example and assume that from this new arrival will emanate 9,000,000 more. However, against this expectation of the mean lifetime reproduction, we balance the knowledge that 99.9% of such arrivals will fail to survive to reproductive age (e.g., Clark et al. 1998*b*). If mortality rates are high, then the bulk of these events amount to naught. Faced with the importance of extreme dispersal, how do we gauge the impact of these rare dispersal events when reproductive variability is high?

Here, we provide a solution to the problem of spread that incorporates fat-tailed dispersal and variance in R_0. Our alternative approach is motivated by two observations from previous efforts. First is the fact that the fatter the tail the more extreme become the distances between the remote colonists and the population interior (Mollison 1972; Kot et al. 1996; Lewis 1997). Second is the dominant role assumed by net reproductive rate as the tail becomes increasingly flat (Clark 1998). As the tail flattens, the density of propagules at distance tends to scale directly with R_0.

Our approach helps resolve the contradiction between infinite moments of kernels fitted to data and the finite moments of the data themselves, and we integrate the variability that results from differential longevity (and, thus, R_0). We demonstrate how spread based on extreme dispersal events can accommodate the dominant effect of R_0 without resorting to the details of population growth. We fit parametric models to data as the basis for this analysis, but we focus on moments of extreme events and those that can be generated by discrete sampling from these distributions. Our method is based on sample sizes used by organisms themselves (i.e., R_0). Finally, we determine how the variability in R_0 that results from variable life span affects the velocity of spread. Based on this analysis, we suggest that Holocene spread of trees may have been less rapid than previously predicted by models, and we discuss why.

Theoretical Development

Estimating spread when individuals interact both nonlinearly and stochastically (as they do in the real world) is one of the fundamental challenges to population theory. A finite asymptotic velocity for the location beyond which a fixed density of individuals lies (the "expectation velocity" of Mollison [1977]) results from nonlinear deterministic models if the tail of the dispersal kernel is exponentially bounded. For a nonlinear stochastic process, a finite velocity of furthest-forward individuals (the "furthest forward velocity" of Mollison [1977]) obtains if the kernel has finite variance (Mollison 1972). Between these two conditions lie a large number of fat-tailed dispersal kernels

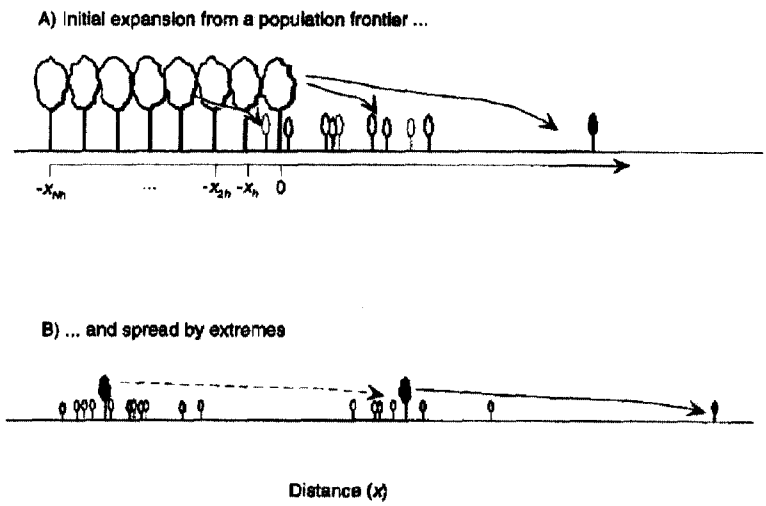

Figure 1: Spread from the frontier of a population (*A*) and, later, by remotely dispersed individuals (*B*)

that yield an asymptotically infinite velocity for a deterministic nonlinear model (Kot et al. 1996) but a finite furthest-forward velocity for a nonlinear stochastic process. Here, we propose a method, based on invasion by "extreme events," that corresponds to changes in the location of the furthest-forward individual. The example that follows this background theory uses dispersal kernels fitted to seed rain data that are both fat-tailed and possess infinite variance.

Spread by Extreme Dispersal

The difference between theoretical moments of distributions and those of data result in qualitatively different predictions of population spread. Exponentially bounded kernels can behave like the data used to fit them (Clark et al. 2001): they have all moments finite, and, when embedded in population models, they predict a traveling wave of advance. Fat-tailed kernels and kernels for which some moments do not exist may not behave like the data fitted to those kernels, in the sense that the data have empirical moment-generating functions and finite moments, whereas the fitted kernel does not. This section provides a means for estimating the velocity of spread that results from dispersal patterns that are best fitted by fat-tailed kernels that may possess few finite moments (as few as one).

We define the net reproductive rate, R_0, as the number of offspring that can be expected from an individual at the time of seed release. It can sometimes be convenient to define R_0 as the number of offspring expected following some (density-independent) mortality of juveniles. This is simply a matter of bookkeeping. Because dispersal is typically estimated from seed (rather than seedlings or saplings), our definition of R_0 based on seed is most readily applied to dispersal data. Our model assumes linear population growth up to some finite maximum density, and thus is comparable to traditional (diffusion, integrodifferential, and integrodifference) models of spread. Our application of the model is cognizant of the fact that migrations usually take place in the presence of other species. Our estimates of R_0 are based on field estimates of fecundity and survivorship in a competitive environment. R_0 can be much greater than 1 during an initial advance, as the population increases from low density. Thus, the model has broad relevance to invasion problems, and the specific application here accommodates the measured effects of mortality in actual stands of trees.

Consider a parent that produces an average of R_0 offspring over its lifetime with dispersal described by kernel $f(x)$. If the kernel is sufficiently fat-tailed, and the net reproductive rate, R_0, is sufficiently large, the population can spread as a series of remote subpopulations established by extremely placed offspring (Davis 1987; Lewis 1997; Shigesada and Kawasaki 1997; fig. 1*B*). The distribution of leaps forward might be approximated by the sum of random variates drawn from the distribution of furthest-dispersing propagules, that is, extremes. With a fat tail, there is a good chance that the extremely placed individual will find itself distant from the population frontier or even from the next closest disperser. This dislocation means that the extremely placed individual becomes the basis for additional spread. Unlike a diffusing population, the expanding "front" is not supported by a large, nearby pop-

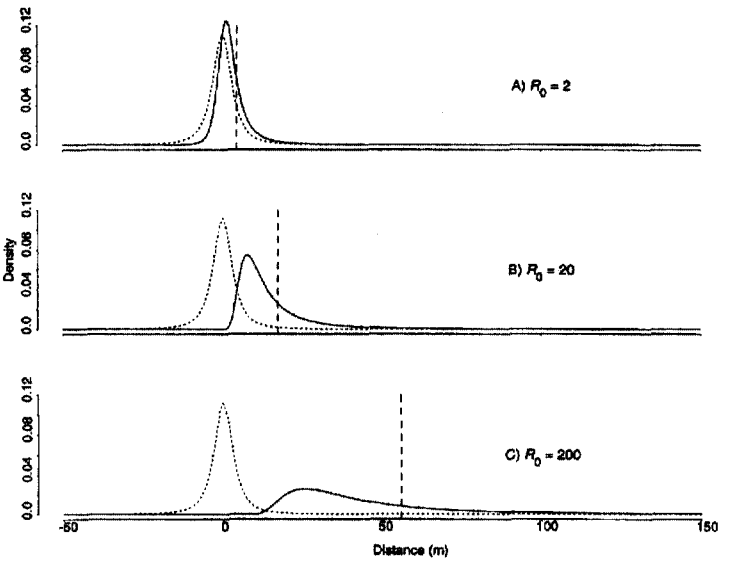

Figure 2: The relationship between the dispersal kernel $f(x)$ (*dashed line*, eq. [10]) and the density of extreme dispersers $p(x; 1)$ for three different net reproductive rates: $R_0 = 2$ (*A*), $R_0 = 20$ (*B*), $R_0 = 200$ (*C*). The vertical dashed line marks the expected extreme disperser (eq. [12]).

ulation (e.g., a traveling wave). To estimate spread, we can avoid the complexity of previous approaches by concentrating on the extremes. Here, we derive this distribution of extreme dispersal for a parametric kernel as basis for estimating rate of spread.

Let $p(x; N)dx$ be the probability that the furthest-dispersing individual from a group of N evenly spaced parents settles on the interval $[x, x + dx]$. The probability density function (PDF) for a seed that arises from a single parent is the product of the events that a seed settles at x and all other seeds from the parent settle closer to the source:

$$p(x; 1) = R_0 f(x)\left[\int_{-\infty}^{x} f(y)dy\right]^{R_0-1} \qquad -\infty < x < \infty, \quad (1)$$

where $f(x)$ is the dispersal kernel (also a PDF). The factor R_0 in equation (1) is the number of ways in which we can obtain a given outcome (any one of R_0 total offspring can be the extreme case). The "1" in $p(x; 1)$ refers to extreme dispersal from a single parent plant to distinguish this distribution from one derived for the edge of a continuous population (see below).

We arrive at the same density starting from the probability that the extreme disperser lies to the left of a point located distance x to the right of the parent, that is, the cumulative distribution function (CDF):

$$P(x; 1) = \left[\int_{-\infty}^{x} f(y)dy\right]^{R_0} = [F(x)]^{R_0}, \quad (2)$$

where $F(x)$ is the CDF for the dispersal kernel $f(x)$. Differentiation yields the PDF for the furthest-forward disperser:

$$p(x; 1) = R_0 f(x)[F(x)]^{R_0-1}, \quad (3)$$

which is equivalent to equation (1). The development of equations (1)–(3) can be viewed as an application of order statistics, with $P(x, 1)$ being the sampling distribution of the R_0th quantile (e.g., Stuart and Ord 1994).

The density of extremes incorporates the contributions of both the dispersal kernel and the net reproductive rate, R_0 (fig. 2). Net reproductive rate has a dramatic effect on the extremes. With $R_0 = 2$, extreme dispersal does not much exceed the kernel itself (fig. 2*A*). With $R_0 = 200$, the extremes extend well beyond the dispersal kernel (fig. 2*C*).

Extremes Derived from the Continuous Population

Upper and lower bounds on population spread per generation, c, can be derived under differing assumptions on distribution of the parent population. Spread by leaps from one extremely placed colony to the next (fig. 1*B*) approx-

imates migration far from a population center. A lower bound c^- comes from assuming that the only possible parent for the furthest-forward individual is the furthest-forward individual from the last generation. Initially, spread could commence from the edge of a continuous population, supported by the large nearby seed source (fig. 1*A*); fat-tailed dispersal subsequently shifts the process to spread by extremes (fig. 1*B*). As discussed below, an upper bound c^+ comes from assuming that the possible parents for the furthest-forward individual occupy a closed stand at density $1/h$ (fig. 1*A*) for crown size h. Abundant seed means that the initial spread from a continuous population can be more rapid than the rate that prevails later, when spread is perpetuated by scattered individuals. If we assume that spread commences from the edge of a continuous population (fig. 1*A*), and that fat-tailed dispersal subsequently shifts the process to spread by extremes (fig. 1*B*), then c^+ and c^- suggest initial and asymptotic spread rates for the population. This interpretation in terms of initial and final spread rates is not proved mathematically. Here, we derive the initial spread depicted in figure 1*A*. As shown below, our estimates for "initial" rates and "eventual" rates give upper and lower bounds for population spread rate.

Consider a transect perpendicular to a population frontier, where seed source is distributed more or less evenly to the left of the front at $x = 0$ (fig. 1*A*). The population spreads to the right at an initial rate determined by offspring that can originate from parents located anywhere to the left of $x = 0$ (i.e., $x \leq 0$). Density dependence is implicit because the continuous population is constrained to have an upper limit on seed production (and canopy coverage) at density $1/h$. The parameter h can be viewed as the distance between individual trees, and Nh is the linear extent (width) of the population. Seed production is distributed at locations along the transect $(-x_{Nh}, \ldots, -x_h, 0)$.

Assuming that individuals each produce R_0 offspring, the probability that the extreme disperser travels no further to the right than x is the CDF

$$P(x; N) = \prod_{k=0}^{N} [F(x + x_{hk})]^{R_0}.$$

Note that equation (2) is the special case where $N = 1$. The corresponding PDF is

$$p(x; N) = \sum_{k=0}^{N} p_k(x; N), \tag{4}$$

where

$$p_k(x; N) = \frac{R_0 f(x + x_{hk}) P(x; N)}{F(x + x_{hk})}.$$

Here, each $p_k(x; N)$ is associated with the event that the individual at location $-hk$ produces the extreme offspring. To see this more clearly, observe that

$$p_k(x; N) = R_0 f(x + x_{hk})[F(x + x_{hk})]^{R_0 - 1} \times \prod_{j \neq k}^{N} [F(x + x_{hj})]^{R_0}.$$

The first part of this expression is equation (3), describing extreme dispersal from location x_{hk}. The product series that follows is the cumulative probability that offspring deriving from all other $N - 1$ locations do not travel beyond x. Note that, for $N = 1$, equation (4) collapses to equation (3).

As expected, a large population center has greater extreme dispersal distances than does an isolated individual. The dispersal kernel for *Acer rubrum* (*dashed line*, fig. 3*A*) has a density of extremes ($N = 1$ in fig. 3*A*) with a mean value of 230 m per generation. This increases to 430 and 530 m per generation for $N = 5$ and $N = 10$, respectively.

Velocity of Spread

If spread is controlled by extreme dispersal estimated as a parametric kernel, then the distribution of rates of spread is the sum of random draws from $p(x; N)$. The most straightforward solution to the distribution of sums obtains from characteristic functions. Unfortunately, characteristic functions for many fat-tailed densities (including one applied to seed dispersal below) cannot be inverted, and many (also including ours) possess infinite moments. Thus, while the density (eq. [1] or [4]) provides a description of extreme dispersers, it may not help us estimate spread; the fitted model may lack finite moments, whereas the data have all moments finite.

Although we may be unable to evaluate moments for a parametric kernel, equations (1), (3), and (4) provide a simple tool for estimating moments of data fitted to a parametric kernel $f(x)$. Indeed, this is the typical problem faced when estimating spread: dispersal data are summarized and reported from a fitted parametric model, and we wish to estimate how fast the population might expand given the true number of offspring produced, that is, R_0. A distribution of extremes is readily constructed from the most distant propagule that arises from a random sample of size R_0 drawn from the parametric kernel (fig. 4). Thus, equations (1), (3), and (4) provide for simulation that accommodates both the kernel shape and the sample size employed by the parent, that is, R_0.

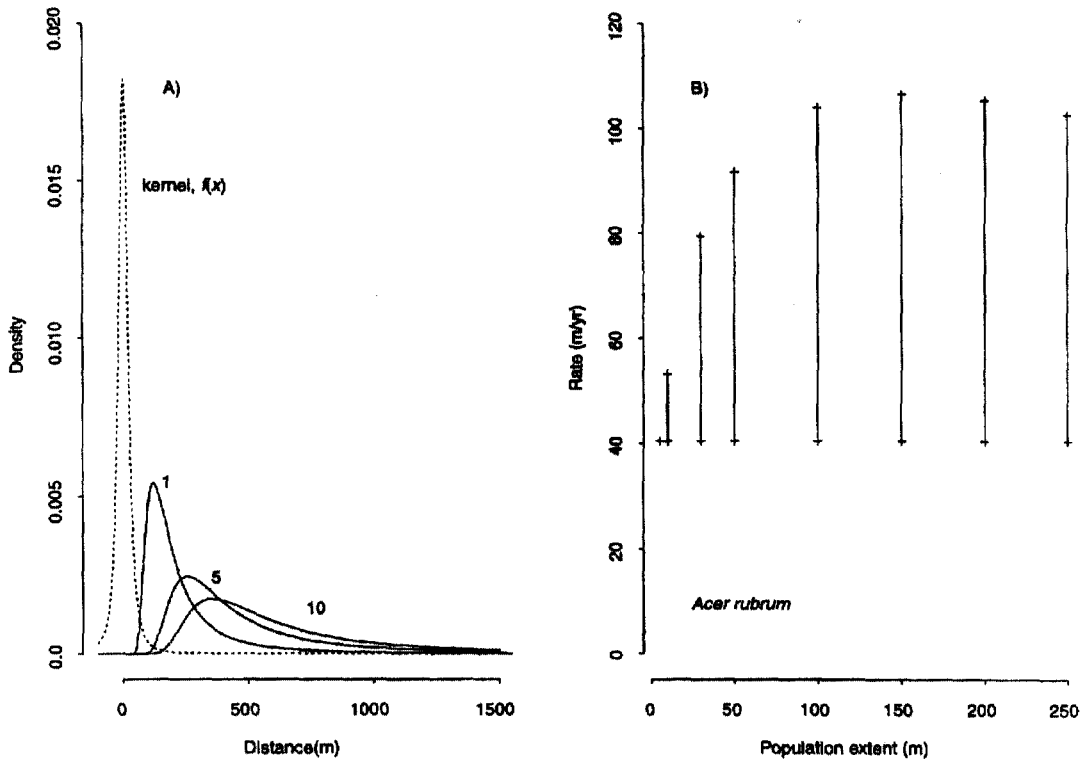

Figure 3: *A*, *Acer rubrum* dispersal kernel $f(x)$ (*dashed line*) and densities of extreme dispersal $p(x; N)$ for three values of N. *B*, Maximum and minimum rates of spread for different resident population sizes from equation (6). Population extent is equal to the number of trees N times the distance along the transect (fig. 1*A*) per tree (taken here to be $h = 5$ m). The upper bound approaches an asymptote with increasing population extent. The minimum value (for $N = 1$) is plotted for reference, bounding a potential range of rates that might prevail over time.

An upper bound on the rate of spread c^+ follows from the assumption that possible parents for the furthest-forward individual are packed at maximum density (crown size) h (fig. 1*A*). A lower bound c^- follows from the assumption that spread proceeds from one furthest-forward individual to the next (fig. 1*B*). Migrations such as those of temperate forest trees following the rapid warming at the end of the Pleistocene potentially commence from continuous populations, implying a large nearby seed source (fig. 1*A*). Fat-tailed dispersal subsequently shifts the process to spread by extremes (fig. 1*B*). Although c^+ and c^- may approximate initial and asymptotic spread rates for the population, we have not proved this.

The mean rate of spread is the expectation of C, where $C = X/T$, that is, an extreme value for X scaled by generation time T. The density of C is

$$g(c; N) = p(x; N)\left|\frac{dx}{dc}\right| = p(cT; N) \times T, \qquad (5)$$

that is, the density of extreme distances scaled by generation time. We calculate two expectations. A high and transient rate c^+ is associated with spread from a continuous front (fig. 1*A*) and obtains from equation (4). A lower rate c^- is approached as the pattern shifts to one of extremes (fig. 1*B*), obtained from equation (3). We expect the eventual "asymptotic" spread rate to lie between c^+ and c^-, but close to c^-. The expectation is

$$E[C; N] = \frac{1}{T}\int_{-\infty}^{\infty} xp(x; N)dx = \int_{-\infty}^{\infty} cg(c; N)dc. \qquad (6)$$

The lower bound for spread is $c^- = E[C; 1]$, and the upper bound is $c^+ = E[C; \infty]$.

The dispersal kernel for *A. rubrum* (*dashed line*, fig. 3*A*), with a mean value of 230 m per generation, translates to a rate of spread of 40 m yr^{-1} (fig. 3*B*). A small population that might occupy, say, a riparian zone (five to 10 crowns wide; fig. 3*A*) has an average rate of spread of 70–90 m yr^{-1} (population extent of $Nh = 5$ to $10 \times 5 = 25$ to 50, fig. 3*B*). The mean rate approaches 100 m asymptotically as N becomes large (fig. 3*B*). Thus, potential rates of spread

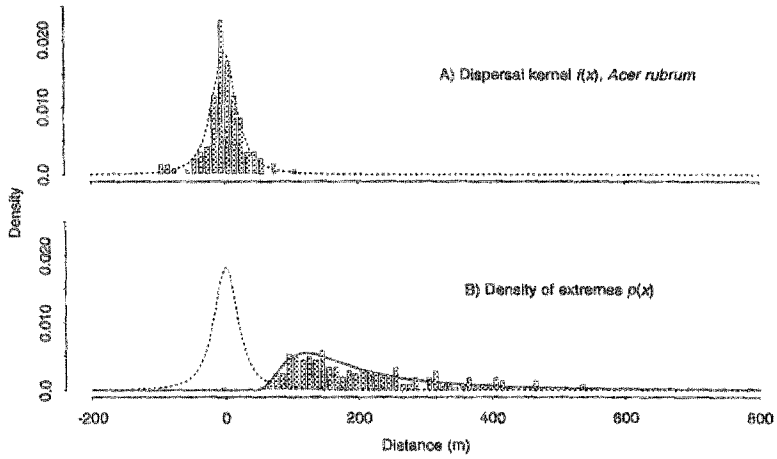

Figure 4: Estimating spread from extreme dispersers. A fat-tailed parametric kernel (eq. [10]) is fitted to *Acer rubrum* dispersal data (Clark et al. 1999). A random sample of R_0 seeds is given by the histogram in (*A*) and compared with the fitted density. Repeated draws from $f(x)$ of size R_0, each time recording the extreme individual, provides a histogram corresponding to $p(x; 1)$, but, unlike $p(x; 1)$, the discrete sample has all moments finite (*B*). Although the parametric kernel in *B* cannot be used to estimate variances, the random sample can.

suggested by the dispersal kernel range from 40 to 100 m per generation, the high value being a closer initial estimate, and the low value expected later on.

Reproduction as an Extreme

The foregoing analysis follows tradition in that it treats reproduction as a fixed value. For many organisms, the very act of reproduction is extremely unlikely. Even for populations experiencing positive population growth rates ($R_0 > 1$), the vast majority of individuals may contribute no offspring to the next generation. Examples include most plants (Clark et al. 1998*a*), birds (Lande 1987), and sea turtles (Crouse et al. 1987). Thus, R_0 represents an average over a large number of zeros and a small minority that do indeed produce offspring. The zeros are those individuals censused at seed or seedling stages that do not survive to reproductive age. Here, we recast the standard life-history equation to accommodate this reproductive variability among individuals, and we propagate that variability to the density of dispersal distances. In other words, we translate reproductive variability into variability in spread. To insure that we do not exaggerate the impact, we use a highly conservative estimate of variance. We include only the variance implicit to the standard life-history equation itself, that is, that which results from variable life span described by the survivor function. In practice, there will be many more sources of variance in R_0 than we include here.

Let R be a random variable representing the reproductive rate with PDF $q_{R_0}(R)$. The many individuals that fail to reproduce represent a class at $R = 0$, and those that do reproduce comprise the "tail" of this density. This density of R values controls population spread because the probability that a seed travels far increases nonlinearly with offspring production (eqq. [1], [3], and [4]). For this analysis, we focus on the situation in figure 1*B* ($N = 1$). Equations (1) and (3) are now conditional densities, and the density of extreme dispersers is obtained by integration:

$$p(x; 1) = \int_0^\infty Rf(x)[F(x)]^{R-1} q_{R_0}(R)\,dR. \tag{7}$$

Because we restrict variability to that caused by differential longevity, net reproductive rate is fully determined by age of death. An individual that dies at age $a = \delta$ produces offspring

$$R(\delta) = \int_0^\delta b(a)\,da, \tag{8}$$

where $b(a)$ is the fecundity schedule. Age of death is described by $f(\delta)\,d\delta$, the probability that death occurs on the age interval $\delta < a < \delta + d\delta$, and is the derivative of the survivor function $S(a)$. The density of net reproductive rates is obtained with the variable change

$$q_{R_0}(R) = f(\delta)\left|\frac{d\delta}{dR}\right| = \frac{f(\delta)}{b(\delta)}. \tag{9}$$

The effect of this variable reproduction on rate of spread

can be determined using the integral equation (7) along with equations (5) and (6).

Methods

Using the Fitted Kernel

To illustrate how variability influences model predictions, we examined the effects of extreme reproduction and dispersal on potential rate of spread using demographic data from southern Appalachians trees. Data sets and parameter estimates are obtained from long-term monitoring and experiments (Clark 1998; Clark et al. 1998*b*, 1999). Use of this data set is not intended as a full analysis of dispersal and invasion; a broader description of dispersal and life history for these species is contained in Clark (1998). The dispersal kernel is a bivariate Student's t (2Dt), which Clark et al. (1999*b*) derived as a continuous mixture of Gaussian densities with dispersal parameter distributed as inverse χ^2. It fits dispersal data better than do the traditional exponential or Gaussian kernels. With Clark et al.'s (1999*b*) shape parameter of $p = 1$, the marginal density in one dimension is

$$f(x) = \frac{1}{2\sqrt{2u}\left(1 + \frac{x^2}{2u}\right)^{3/2}}. \tag{10}$$

The mean is finite, but all higher moments are not. For the estimates that follow we assume that $R_0 \gg 1$ and, consequently, that $R_0/2$ seeds move to the right. This assumption allows us to change the lower integration limit in equation (1) from $-\infty$ to 0, thus permitting an analytical solution for rate of spread. This is a close approximation for large R_0 because the chances that the farthest disperser to the right is less than $x = 0$ is small. Conditioned on the event that a seed travels to the right (positive x), the expected dispersal distance is $E[X] = (2u)^{1/2}$. If R_0 is large, then approximately $R_0/2$ seeds move to the right (positive x) with density

$$p_r(x;\ 1) = \frac{R_0 x^{(R_0/2)-1}}{u^{R_0/4}\left(2 + \frac{x^2}{u}\right)^{(R_0/4)+1}}, \tag{11}$$

and the lower bound on the spread rate is $c^- = E[C;\ 1] = 1/T\int_0^\infty x p_r(x;\ 1)dx$. With the substitution $z = x^2/2u$, we can write this integral in terms of a beta function

$$\begin{aligned} E[C;\ 1] &= \frac{\sqrt{u}R_0}{2T}\int_0^\infty \frac{z^{(R_0/4)-1/2}}{(1+z)^{(R_0/4)+1}}dz \\ &= \frac{\sqrt{u}R_0}{2T}\mathrm{B}\left(\frac{R_0}{4} + \frac{1}{2}, \frac{1}{2}\right) \\ &= \frac{\sqrt{2\pi u}\Gamma\left(\frac{R_0}{4} + \frac{1}{2}\right)}{T\Gamma\left(\frac{R_0}{4}\right)} \approx \frac{1}{T}\sqrt{\frac{\pi u R_0}{2}}, \end{aligned} \tag{12}$$

where $\mathrm{B}(\cdot,\cdot)$ and $\Gamma(\cdot)$ are beta and gamma functions, respectively. The variance and all higher moments are not finite. The approximation used in the last step of equation (12) comes from the asymptotic relationship

$$\lim_{R_0\to\infty}\left[\frac{\Gamma\left(\frac{R_0}{4} + \frac{1}{2}\right)}{\Gamma\left(\frac{R_0}{4}\right)}\right] \to \frac{R_0}{2}.$$

In fact, this limiting result, if approached rapidly, provides useful estimates for values of R_0 as low as 5.

Relaxing the assumption that one-half of all seeds move to the right still permits a solution for the PDF (i.e., using eq. [2]):

$$\begin{aligned} p(x;\ 1) &= R_0 f(x)\left[\frac{1}{2} + \int_0^x f(y)dy\right]^{R_0-1} \\ &= R_0 f(x)\left[\frac{x + \sqrt{2u + x^2}}{2\sqrt{2u + x^2}}\right]^{R_0-1}, \end{aligned} \tag{13}$$

but we were unable to obtain a solution for the mean rate of spread. Provided R_0 is not small, numerical solutions are approximately equal to equation (12).

To determine variances on rates of spread and to evaluate our estimates based on parametric assumptions (i.e., eq. [13]), we sampled directly from equation (10). To simulate spread in one dimension, we rescaled and integrated the 2Dt model fitted to two-dimensional data (Clark et al. 1999*b*). We drew R_0 random t variates from a standard one-dimensional t distribution with $\nu = 2p$ degrees of freedom. We then set sample distances $x_i = (u/p)^{1/2} \times t_i$ to obtain one-dimensional spread scaled to our parameter estimates (recall $p = 1$).

Figure 4 shows $f(x)$ and $p(x;\ 1)$ for *Acer rubrum* data. The sample in figure 4*A* of size $R_0 = 117$ has an extreme disperser at approximately 200 m. A large number of samples of size R_0 produce a distribution of extreme values, represented as a histogram in figure 4*B* that is compared with the parametric $p(x;\ 1)$.

Variable Reproduction

The effect of variable reproduction was evaluated using data sets and the approach of Clark (1998). Assume that trees grow with an approximately constant annual diameter increment g and that seed production is proportional to (β times as great as) basal area (Clark et al. 1998, 1999*b*; Wyckoff and Clark 2000). Then the fecundity schedule is $b(a) = \pi\beta(ga/2)^2$, and net reproductive rate is obtained from equation (8), $R(\delta) = (\pi\beta g^2/12)(\delta^3 - t_1^3)$, where t_1 is maturation age.

Mortality is summarized by a survivor function $S(t_1)$ that determines a probability of surviving to maturation age t_1 and a constant mortality rate ρ thereafter. The density of deaths is

$$\begin{cases} 1 - S(t_1) & \delta < t_1 \\ \dfrac{S(t_1)\rho e^{-\rho(\delta - t_1)}}{1 - e^{-\rho t_2}} & \delta > t_1 \end{cases}.$$

The density of reproductive rates is obtained using equation (9):

$$q_{R_0}(R) = \begin{cases} 1 - S(t_1) & R = 0 \\ \dfrac{4S(t_1)\rho \exp\{-\rho[D(R) - t_1]\}}{\pi\beta[gD(R)]^2(1 - e^{-\rho t_2})} & 0 < R < R(t_2) \end{cases}, \quad (14)$$

where $D(R) = [(12R/\pi\beta g^2) + t_1^3]^{1/3}$ is the inverse function $R^{-1}(\delta)$. The combined effects of extreme dispersal and variable reproduction were determined by substituting equations (11) and (14) in equation (7) and integrating numerically.

Results

The Effect of Extreme Dispersal

Our approach predicts a pattern of spread that might be viewed as a hybrid of previous methods. The example using parameter values for *Acer rubrum* shows a constant average rate (fig. 5*A*, 5*B*), as occurs with simple diffusion models. The pattern differs from diffusion in that spread proceeds as a series of irregular leaps (fig. 5*B*). These most extreme dispersers are peak values in figure 5*B* and represent the formation of distant centers for additional spread. Although the long-term rate of spread approaches a constant expectation, which is predicted by equation (12) (*dashed line*, fig. 5*B*, 5*C*), that rate is much greater than would occur by diffusion. The mean spread rate of 40 m yr^{-1} in figure 5 contrasts with 10 and 20 m yr^{-1} predicted by Gaussian and exponential dispersal kernels, respectively,

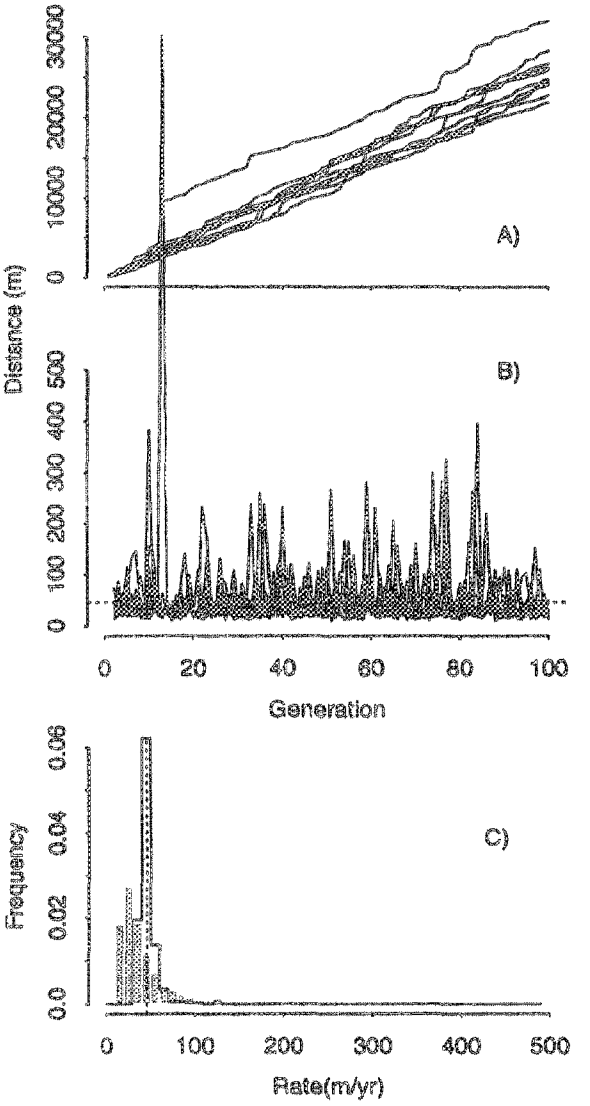

Figure 5: Simulated spread from extreme dispersal for *Acer rubrum*. *A*, Cumulative distance traveled over successive generations for 10 simulations. *B*, Distances traveled by generation for the 10 simulations in *A*. *C*, Comparison of distribution of extreme dispersal events from *B* (*shaded bars*) and the long-term (100 generations) distribution of rates $g(c)$ (*step curve*). The dashed line in *B* and *C* is the expectation from equation (12). The distribution of extreme events is skewed, as predicted by equations (1) and (11). The distribution of rates approaches normality with increasing numbers of generations. The distribution of rates has a mean of 45.4 ± 7.70 m yr^{-1} with 95% of values on the interval (36.1, 64.2). Units in *C* (m yr^{-1}) are obtained by scaling for generation time (eq. [6]).

fitted to the same data. Whereas the fitted kernel used to simulate spread in figure 5 has infinite variance, the simulations provide a finite variance for a distribution of rates that is asymptotically normal (fig. 5*C*). This distribution

corresponds to $g(c;1)$ in equation (5). Moreover, the average rate of spread from simulation agrees with the mean of the distribution of extremes; the estimate from equation (11) is shown as a dashed line in figure 5*B* and 5*C*. We prove this rate to be finite for all relevant assumptions in the appendix.

Although net reproductive rate has a minor effect on the rate of diffusion (for a Gaussian kernel, the rate is proportional to the square root of the log of R_0), the density of extremes captures its dominant effect on fat-tailed spread. For a species with low R_0 and short dispersal distances, such as *Carya*, the most extremely placed seed only reaches 5–50 m (fig. 6*A*). By contrast, wind-dispersed types produce many small seeds, and the extreme disperser might travel 10^2–10^4 m (fig. 6*B*). In the case of *Betula*, the extreme disperser is predicted to always exceed 500 m. The densities of extreme dispersal (fig. 6) predict rates of spread that range over two orders of magnitude (fig. 7). Wind-dispersed types (*Betula, Acer, Liriodendron*) have highest rates (30–80 m yr^{-1}); animal-dispersed types (*Cornus, Nyssa, Carya*) have low rates (0.1–1 m yr^{-1}), depending on N.

The Effect of Variable Reproduction

Variable reproduction slows rates of spread using our parameterizations for tree populations. Figure 8*A* shows a typical density (*A. rubrum*) of net reproductive rates. The density is represented on a log-log plot because the tail would otherwise be obscure. The assumption that 1 in

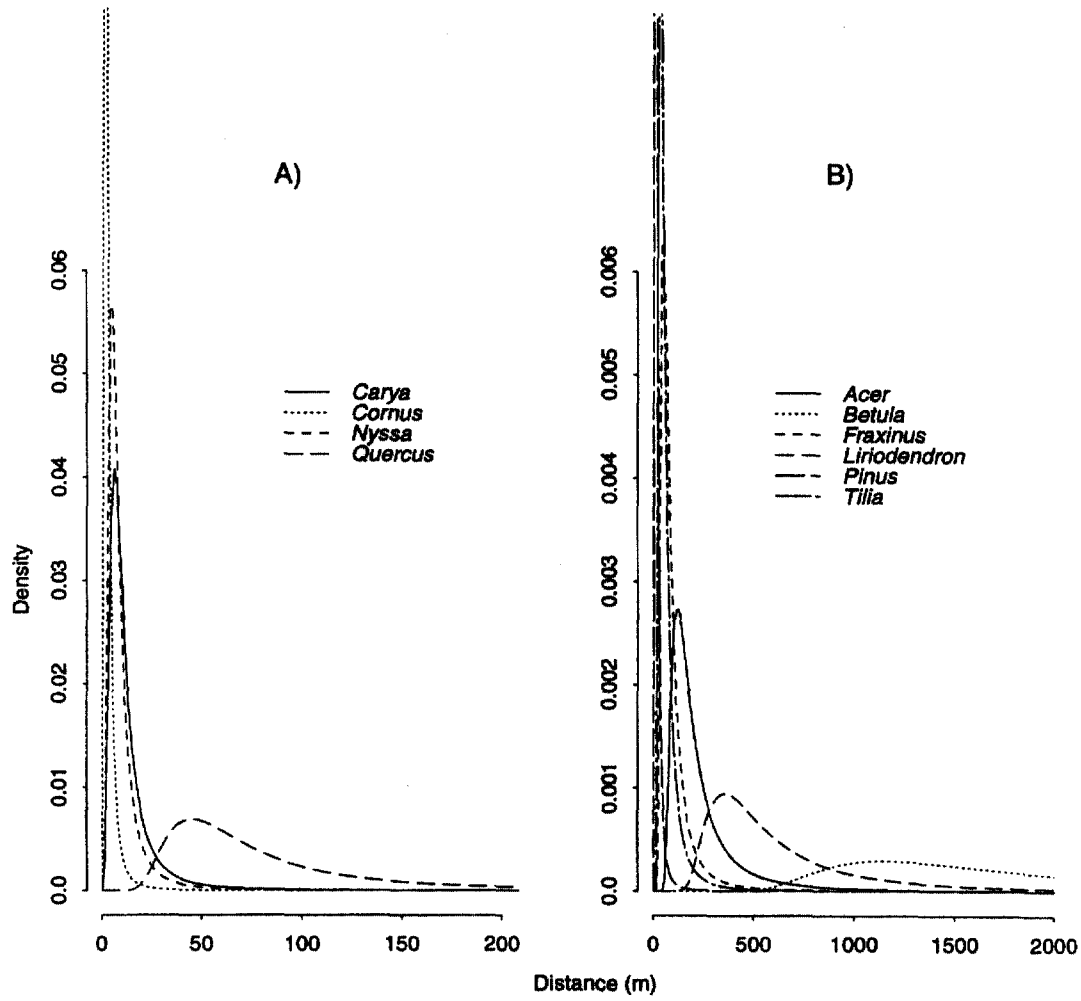

Figure 6: Densities of extreme dispersers for animal-dispersed (*A*) and wind-dispersed (*B*) types from equation (11). Note different scales for horizontal axes.

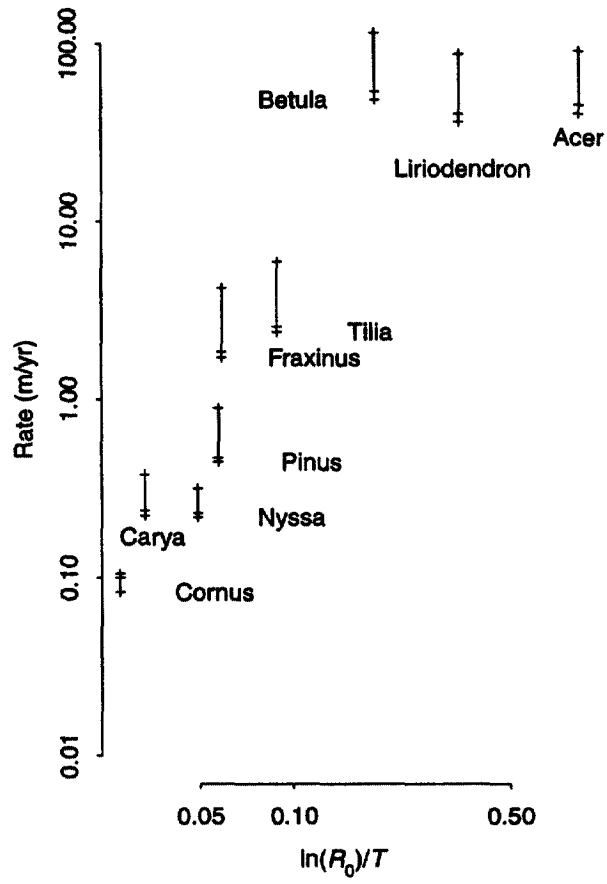

Figure 7: The ranges of spread rates plotted against rates of increase $\ln(R_0)/T$ estimated from dispersal and life-history data for southern Appalachian trees. A range is given for each taxon that has upper and lower bounds that are numerical estimates. The interior tick mark is the analytical result from equation (12).

1,000 seeds reach reproductive age is within the range we observe in modern forests (Clark et al. 1998). This high juvenile mortality is represented by the bulk of the density (99.9%) at the low extreme of figure 8*A*. The remaining tail contains 0.001 (the probability of at least some reproduction).

The two densities of extreme dispersal in figure 8*B* demonstrate the effect of variable recruitment. The upper curve is the density that results from a constant R_0 (eq. [11]). The lower curve is the density that accommodates variance in R_0 (eq. [7]). This density is lower than that for constant R_0 because it includes a large zero class corresponding to the bulk of the R_0 values that equal zero (for clarity, this zero class is not shown). The large zero class means that the overall expectation of extreme dispersal is much lower than predicted for a constant R_0. Thus, although both densities assume the same mean R_0, variation of the type caused by high juvenile mortality slows the rate of spread.

For juvenile survivorship of 0.001, variable R_0 profoundly limits the rate of spread estimated from our dispersal data. We found that invasion progressed two orders of magnitude slower for variable R_0 than it did for constant R_0 (fig. 9*B*). Poorly dispersed species are predicted to spread on the order of meters per century. Increasing the rate of spread requires much higher juvenile survivorship ($S(t_1)$ in eq. [14]), which results, in turn, in higher R_0.

Application to Contemporary Spread

There are few examples of contemporary tree invasions for which estimates of life history, dispersal, and invasion rates are available. Dispersal estimates and invasion rates for two spruce (*Picea*) species in Alaska allow for model application. We combined dispersal estimates obtained from a remnant white spruce stand into a surrounding clearcut with rates of Sitka spruce spread into Glacier Bay.

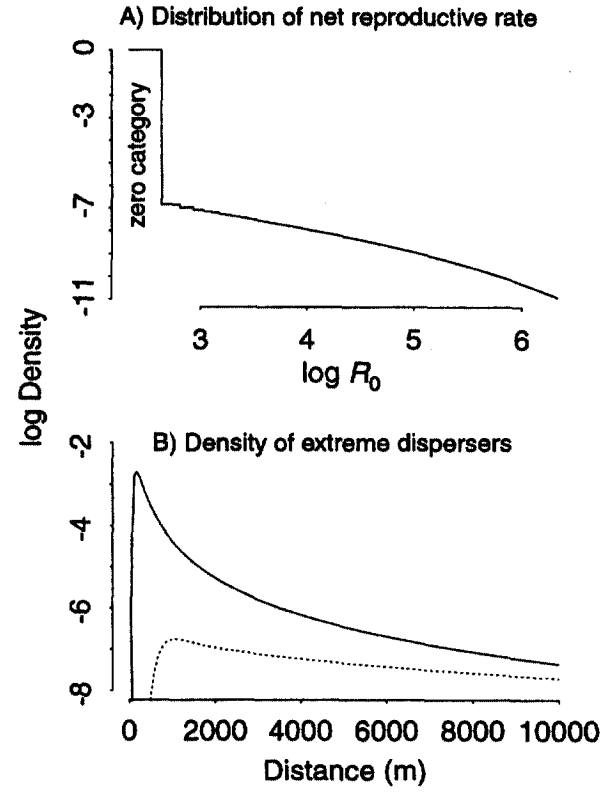

Figure 8: Density of net reproductive rates (*A*) and comparison of extreme dispersal kernels for constant and variable R_0 (*B*). The upper curve in *B* assumes the mean value for R_0, and the lower curve in *B* integrates the full density of R_0 values shown in *A*. Parameters are for *Acer rubrum*.

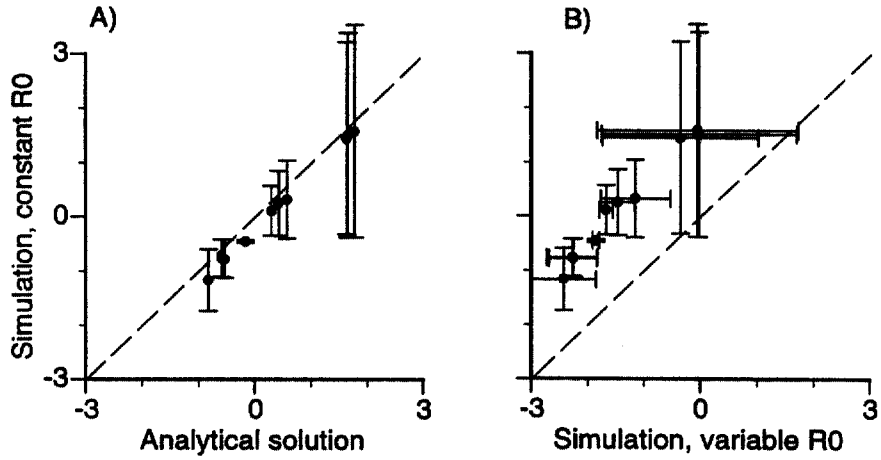

Figure 9: Comparisons of spread rates. *A*, Simulation results (*vertical axis*) agree with the analytical model (*horizontal axis*) summarized by the mean (eq. [12]). *B*, Rates of spread that include the full density of R_0 values from equation (7) (*horizontal axis*) are consistently lower than are those that assume the mean R_0 (eq. [6]). Both axes are log values.

Fastie (1995) found that the rate of spread into deglaciated terrain depended on distance to the closest seed source, with rates averaging from 300 to 400 m yr^{-1}. To estimate a dispersal kernel, we used seed trap data from transects emanating from the remnant stand (S. Rupp, unpublished manuscript). Our maximum likelihood approach assumes a seed source that is everywhere constant within the stand, and seeds are dispersed in all directions according to a 2Dt kernel (Clark et al. 1999). The mean of the Poisson sampling distribution is given by the 2Dt kernel integrated over the source area. Dispersal parameters from nine transects averaged $u = 5{,}531 \pm 3{,}024$ m^2. Because we lack full life-history data, we considered the range of R_0 values (5,000–50,000) we obtain for tree species having wind-dispersed seed and having fecundity rates similar to those estimated here (Clark 1998). The geometric mean value for this range is 16,000. We further assume $T = 50$ yr (Fastie 1995), the maximum likelihood estimates for u from our nine transects, no covariance in u and R_0, and a standard error on R_0 of 1,000. We bootstrapped spread rates using equation (12). The bootstrap is thus parametric in R_0 and nonparametric in u.

The distribution of bootstrapped estimates straddles Fastie's (1995) estimate based on stand reconstruction (fig. 10). The skewed pattern of spread rates results from a limited number of u parameter estimates with uncertainty resulting from a limited number of sample years. The broad range of estimates is consistent with the prediction of highly variable rates, yet the central tendency is close to the observed rate. Our data underestimate the rate of spread, but we expected an underestimate because we used the lower estimate of c^-, and some seed might travel from distant, continuous stands.

Discussion

Spread predictions that ignore variance contain order of magnitude bias. Our solution to the problem of spread that results from fat-tailed dispersal provides two new insights that depart from former views. First, we demonstrate that spread is intermediate in character and in rate between simple diffusion and fat-tailed dispersal predicted by previous models. Second, we show that reproductive variability can have a profound effect on the rate of spread.

Dispersal Is Discrete

Previous results showed that velocities predicted from mean dispersal distances (i.e., diffusion) are qualitatively and quantitatively inaccurate (Mollison 1972; Kot et al. 1996; Lewis 1997; Clark 1998), but analyses from fat-tailed kernels produce no asymptotic estimate; spread just accelerates indefinitely (Kot et al. 1996). By acknowledging that individuals are discrete, we obtain estimates of spread that are faster and noisier than diffusion but still finite (fig. 5). Our simulation method that uses the same "sample size" as a parent (i.e., R_0) allows calculations of means, variances, and so forth. The analytical calculation for the mean agrees with simulation (fig. 9*A*). The simple approximation represented by equation (12) provides a rule of thumb that can be readily estimated from a fitted kernel. The approach can be implemented in the common situ-

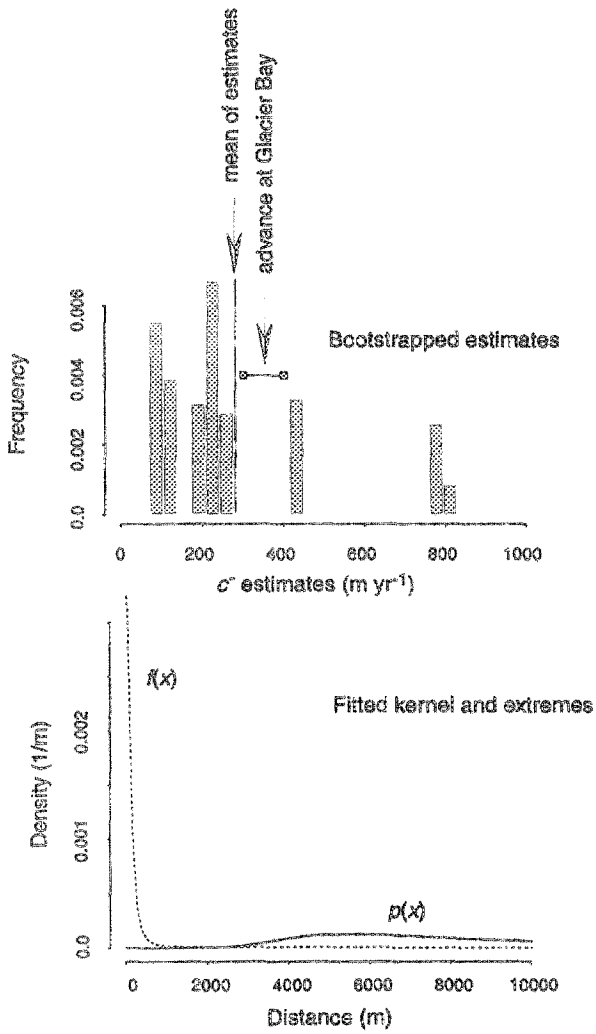

Figure 10: Estimates of spread (A) bootstrapped from the fitted dispersal kernel $f(x)$ shown for the mean value of parameter u in B. The corresponding extreme density in B uses a value of $R_0 = 16{,}000$.

ation where a fitted kernel is available, and raw data are not.

Our contribution here is about analyzing data, not about fitting them. Spread rates estimated by our method are no better than the data used to fit them, and kernel tails are hard to estimate. However, once we have dispersal information, we have had no way to use it, nor have we had ways to analyze consequences of dispersal scenarios that might have prevailed in the past or will in the future. There are many situations where data are available (examples in Kot et al. 1996; Clark et al. 1999) or where there is need to explore the implications of a dispersal scenario. Our approach permits a direct analysis, whereas previous methods do not.

Any invasion by leptokurtic dispersal is sensitive to the shape of the tail (Kot et al. 1996; Clark 1998). Because the tail cannot be adequately characterized, assuming a parametric, fat-tailed kernel makes for speculative interpretation. However, unlike traditional models, our solution does not "blow up." Our method is much less susceptible to errors in the tail because a random sample of size R_0 from a kernel fitted to data produces a simulated data set much like the original data (fig. 4). The infinite tail that controls the predictions of parametric models does not contribute to the discrete samples drawn from such densities. By acknowledging that propagules are discrete, we avoid the extreme sensitivity to tail shape that makes traditional models unsatisfactory.

The effect of R_0 can be appreciated by comparing the order of spread rate. With traditional diffusion (dispersal distance x has the Gaussian kernel $x \sim N(0, \sigma^2)$), the velocity has order $O(\ln R_0)^{1/2}$. A fat-tailed kernel that fitted dispersal data of Clark (1998; dispersal kernel $x^{1/4} \sim N(0, \sigma^2)$) has velocity $2t \times O(\ln R_0)^2$, where t is time in generations. In addition to increasing over time, the order shows high impact of fecundity. The extreme value approach applied here shows spread of order $O(R_0)^{1/2}$ (eq. [12]). Not only does it not accelerate, but fecundity effects are intermediate between classical models of diffusion and fat-tailed spread.

Variable Reproduction Slows Invasion

We did not include in our analysis all sources of variability in offspring production, because we focus on the situation where most of the rare, long-distance dispersers fail to reproduce. Previous analyses simply apply the mean net reproductive rate uniformly to all individuals. By focusing on the variability that results from longevity, we include only the variance that is implicit to any calculation of R_0 (eqq. [8], [9]). In other words, we do not assume the process to be more variable than do previous analyses; we just include the variance previous models imply.

Velocities based on mean reproduction are importantly biased because there is huge variance among individuals in their reproductive output, and velocity is very sensitive to offspring production (eq. [2]). For instance, high mortality between seed release and reproductive age means that Skellam's (1951) assumed R_0 of 9,000,000 new seeds emanating from each seed arrival averages over a distribution having several orders of magnitude more seed in a zero class and rare individuals that produce far more than 9,000,000. Abiding the variance in reproduction vastly lowers the predicted velocity. Because many populations are characterized by high juvenile mortality and potentially long life (Crouse et al. 1987; Lande 1987), our results have broad application.

How Does Variability Alter Predictions of Tree Spread?

Clark (1998) used parametric kernels to demonstrate that tree invasions of several hundred meters per year cannot be rejected on the basis of modern dispersal data. However, these highest rates were not obtained by all species due to low fecundity and restricted dispersal. These rates were consistent with predictions of integrodifference equation models after several generations for species that produce large quantities of well-dispersed seed, but the integrodifference model predicts continued acceleration.

Those simulations and results presented here point out that many species may not be capable of such rapid spread. We can never completely rule out the possibility that occasional seeds are transported long distances by birds, thus providing for the remarkably high rates of spread implied by interpretations of fossil pollen data (Davis 1981). But some taxa (e.g., *Carya*) have no known long-distance dispersal vectors, so rapid migration is less plausible. By focusing on the extremely placed seeds, we still obtain rates of spread near 1 m yr^{-1} for *Carya* (fig. 7). Including the variance in R_0 reduces the prediction still farther (fig. 9*B*). Assuming juvenile survivorship substantially greater than today still does not predict rates as high as 10 m yr^{-1}, far lower than inferred from fossil pollen data. Although there may have been unknown dispersal vectors in the past, *Carya* nuts are accessible primarily to rodents, few of which would be expected to transport nuts long distances.

The rates of spread we predict should lead to reconsideration of the notion that Pleistocene true populations may have been more extensive than previously thought. Bennett (1987) suggested that low pollen percentages can derive from scattered tree populations that occupied sites farther north than those used to infer rapid spread. Even relatively small populations in protected sites could support rapid initial spread (fig. 3), and there would have been far less distance to cover if such populations extended to higher latitudes. Increasing evidence that the North American ice sheet blocked winter intrusions of frigid Arctic air (e.g., Wright 1992) means that the minimal low temperatures that control modern northern range limits (Sakai and Weiser 1973; Larcher and Bauer 1981) may not have been so extreme as to completely exclude these taxa. If populations were further north in eastern North America than previously thought, the rates of spread needed to accomplish Holocene spread are closer to the estimates we provide here.

Conclusions

Our results demonstrate that two common kinds of variability in dispersal limit the progress of invasion. One kind of variability (the rare, long-distance kind) does not provide for the unlimited rates of spread that parametric models predict. Once we acknowledge that offspring are discrete, our method provides a means for calculating spread, and it is intermediate between diffusion and parametric fat-tailed spread, both in velocity and in character.

The second kind of variability (the reproductive kind) can profoundly slow rates of spread. By incorporating only the variability implied by the standard R_0 calculation, we demonstrate that differential longevity described by the survivorship schedule predicts slower spread than the assumption that all individuals have identical longevity and produce the mean R_0.

New insights provided here apply to all organisms characterized by iteroparous life histories and/or rare, long-distance dispersal. The example we use (tree expansions at the end of the Pleistocene) suggests dramatic effects of these types of variability and suggests reexamination of Pleistocene distributions and subsequent spread.

Acknowledgments

For their reviews of the manuscript, we thank B. Beckage, D. Hart, J. HilleRisLambers, J. Lynch, J. McLachlan, A. Pringle, L. Stone, and an anonymous reviewer. The research was supported by National Science Foundation grants BSR-9444146, DEB 9453498, DEB-9632854 (J.S.C.), and DMS 9973212 (M.L.).

APPENDIX

Here, we prove dispersal by fat-tailed kernels with infinite moments produces finite rates of spread, provided there are discrete (finite) offspring. We begin with the case depicted in figure 1*B* (spread from isolated individuals). We then consider spread from a continuous front (fig. 1*A*).

Spread from Isolated Individuals

Assume offspring disperse to locations $\eta_1, \ldots, \eta_R$, where R is the number of offspring. The extreme disperser lands a distance from the parent

$$\xi = \max_{1 \le i \le R} \eta_i.$$

Further assume that $\eta_1, \eta_2, \ldots$ are independent, and the $[\eta_i, i \ge 1]$ and R are independent. Let $f(x)$ be the density ($F(x) = \int_{-\infty}^{x} f(x')dx'$, the distribution function) of η_i.

Claim: If $E[R] < \infty$, and $E[\eta_1] < \infty$, then $E[\xi] < \infty$. If $E[\xi] < \infty$, and $\Pr\{R = 0\} < 1$, then $E[\eta_1] < \infty$.

Proof: For the sake of simplicity, we assume that $\eta_i \ge 0$. Then the distribution function of ξ (i.e., eq. [3]) is

$$P(x; 1) = \Pr\left\{\max_{1 \le i \le k} \eta_i \le x\right\} = F^k(x).$$

Thus,

$$E[\xi|R] = \int_0^\infty x dF^R(x) = \int_0^\infty [(1 - F^R(x)]dx,$$

and, therefore,

$$E[\xi] = E\left[\int_0^\infty [1 - F^R(x)]dx\right].$$

Note that, by the mean value theorem,

$$kF^{k-1}(x)[1 - F(x)] \le 1 - F^k(x) \le k[1 - F(x)].$$

Assume that $E[R] < \infty$ and $E[\eta_1] < \infty$. Then

$$E\left[\int_0^\infty [1 - F^R(x)]\right] \le E\left[R \int_0^\infty [(1 - F(x)]\right] = E[R]E[\eta].$$

Assume further that $E[\xi] < \infty$. Because

$$1 - F(x) \le 1 - F^k(x),$$

we have

$$1 - F(x) \le 1 - F^R(x), \quad \text{if } R = 1, 2, \ldots,$$

and, therefore,

$$\begin{aligned}\int_0^\infty [1 - F(x)] \le E\left[\int_0^\infty [1 - F^R(x)]dx\right] &= \sum_{k=1}^{\infty} \int_0^\infty [1 - F^k(x)]dx \times \Pr\{R = k\} \\ &\ge \int_0^\infty [(1 - F(x)]dx \sum_{k=1}^{\infty} \Pr\{R = k\} \\ &= \Pr\{R > 0\}E[\eta_1].\end{aligned}$$

On these conditions: if $\Pr\{R = 0\} = 1$, no offspring; if $\eta \le c$, for some constant c, then for any R,

$$\max_{1 \le i \le R} \eta_i \le c,$$

so $E[\xi] < \infty$; if $E[\xi] < \infty$, then the "edge" is moving with a constant velocity, which is exactly $E[\xi]$.

Spread from a Continuous Front

Let X^+ be the extreme dispersal distance from a population front (fig. 1*A*) with CDF $P(x; N)$. The expectation can be written as

$$E[X^+|R, N] = \int_0^\infty [1 - P(x; N)]dx,$$

where $P(x; N)$ is the CDF corresponding to equation (5). Noting that $P(x; N) \le F(x)$, if

$$\int_0^\infty [1 - P(x; N)]dx < \infty$$

with probability 1, and $\Pr\{R = 0\} < 1$, then

$$\int_0^\infty [1 - F(x)]dx < \infty,$$

that is, the dispersion of each individual has a finite mean.

Now, if $F(1) > 0$, we can assume, without loss of generality, that

$$\int_0^\infty [1 - P(x; N)]dx = \int_0^1 [1 - P(x; N)]dx + \int_1^\infty [1 - P(x; N)]dx$$

$$\le 1 + \int_1^\infty [1 - P(x; N)]dx.$$

Because $1 + x \le e^x$, we have

$$0 \le 1 - P(x; N) = 1 - \exp\left\lfloor R \sum_{k=0}^{N} \ln F(x = x_{kh}) \right\rfloor \le R \sum_{k=1}^{N} [(-\ln F(x + x_{kh})],$$

and, therefore, by change of variable, we have

$$\int_1^\infty [1 - P(x; N)]dx \le R \sum_{k=1}^{N} \int_1^\infty -\ln F(x + x_{kh})dx \le RN \int_1^\infty -\ln F(x)dx.$$

If $1 \le x \le \infty$, then

$$0 < \ln[1] - \ln\{1 - [1 - F(x)]\} \le \frac{1}{F(1)}[1 - F(x)],$$

and, therefore,

$$\int_1^\infty [1 - P(x; N)]dx \leq \frac{RN}{F(1)} \int_1^\infty [1 - F(x)]dx.$$

First, if $\Pr\{R = 0\} < 1$ (there are some offspring), then $E[\eta_1] \leq E[X^+ \mid R]$ (i.e., the extreme disperser from any one parent cannot exceed the extreme distance for all N parents) on the set $R > 0$ and

$$E[\eta_1] \Pr\{R \geq 1\} \leq E[X^+].$$

Hence, if $E[X^=] < \infty$, then $E[\eta_1] < \infty$.

Second, there is a constant $c = c(F)$ such that

$$E[X^+ \mid R] \leq cRN\, E[\eta_1].$$

Thus, if $E[\eta_1] < \infty$, and $E[R] < \infty$, then $E[X^+] < \infty$. (Note: If N is a random variable, then $E[N] < \infty$, $E[R] < \infty$, and $E[\eta_1] < \infty$, implying that $E[X^+] < \infty$.)

Literature Cited

Andow, D. A., P. M. Kareiva, S. Levin, and A. Okubo. 1990. Spread of invading organisms. Landscape Ecology 4:177–188.

Bennett, K. D. 1987. Holocene history of forest trees in southern Ontario. Canadian Journal of Botany 65: 1792–1801.

———. 1998. Why trees migrate so fast: confronting theory with dispersal biology and the paleorecord. American Naturalist 152:204–224.

Clark, J. S., C. Fastie, G. Hurtt, S. T. Jackson, C. Johnson, G. King, M. Lewis, et al. 1998*a*. Reid's paradox of rapid plant migration. BioScience 48:13–24.

Clark, J. S., E. Macklin, and L. Wood. 1998*b*. Stages and spatial scales of recruitment limitation in southern Appalachian forests. Ecological Monographs 68:213–235.

Clark, J. S., M. Silman, R. Kern, E. Macklin, and J. HilleRisLambers. 1999. Seed dispersal near and far: generalized patterns across temperate and tropical forests. Ecology 80:1475–1494.

Clark, J. S., L. Horváth, and M. Lewis. 2001. On the estimation of spread for a biological population. Statistics and Probability Letters 51:225–234.

Crouse, D., L. Crowder, and H. Caswell. 1987. A stage-based model for loggerhead sea turtles and implications for conservation. Ecology 68:1412–1423.

Davis, M. B. 1981. Quaternary history and the stability of forest communities. Pages 132–153 *in* D. C. West, H. H. Shugart, and D. B. Botkin, eds. Forest succession: concepts and application. Springer, New York.

———. 1987. Invasion of forest communities during the Holocene: beech and hemlock in the Great Lakes region. Pages 373–393 *in* A. J. Gray, M. J. Crawley, and P. J. Edwards, eds. Colonization, succession, and stability. Blackwell Scientific, Oxford.

Fastie, C. L. 1995. Causes and ecosystem consequences of multiple pathways of primary succession at Glacier Bay, Alaska. Ecology 76:1899–1916.

Johnson, W. C., and T. Webb III. 1989. The role of blue jays in the postglacial dispersal of fagaceous trees in eastern North America. Journal of Biogeography 16: 561–571.

Kot, M., M. A. Lewis, and P. van den Driessche. 1996. Dispersal data and the spread of invading organisms. Ecology 77:2027–2042.

Lande, R. 1987. Extinction thresholds in demographic models of territorial populations. American Naturalist 130:624–635.

Larcher, W., and H. Bauer. 1981. Ecological significance of resistance to low temperature. Pages 403–437 *in* O. L. Lange, P. S. Nobel, C. B. Osmond, H. Ziegler, eds. Encyclopedia of plant physiology. Springer, Berlin.

Lewis, M. A. 1997. Variability, patchiness and jump dispersal in the spread of an invading population. *In* D. Tilman and P. Kareiva, eds. Spatial ecology. Princeton University Press, Princeton, N.J.

Lubina, J. A., and S. A. Levin. 1988. The spread of a reinvading species: range expansion in the California sea otter. American Naturalist 131:526–543.

Mollison, D. 1972. The rate of spatial propagation of simple epidemics. Proceedings of the sixth Berkeley Symposium on Mathematics, Statistics, and Probability 3: 579–614.

———. 1977. Spatial contact models for ecological and epidemic spread. Journal of the Royal Statistical Society B 39:283–326.

Portnoy, S., and M. F. Willson. 1993. Seed dispersal curves: behavior of the tail of the distribution. Evolutionary Biology 7:25–44.

Sakai, A., and C. J. Weiser. 1973. Freezing resistance of trees in North America with reference to tree regions. Ecology 54:118–126.

Shigesada, N., and K. Kawasaki. 1997. Biologicial inva-

sions: theory and practice. Oxford Series in Ecology and Evolution. Oxford University Press, Oxford.

Skellam, J. G. 1951. Random dispersal in theoretical populations. Biometrika 38:196–218.

Stuart, A., and J. K. Ord. 1994. Kendall's advanced theory of statistics. Arnold, London.

Taylor, R. A. 1978. The relationship between density and distance of dispersing insects. Ecological Entomology 3: 63–70.

Turchin, P. 1998. Quantitative analysis of movement. Sinauer, Sunderland, Mass.

Van den Bosch, F., J. A. J. Metz, and O. Diekmann. 1990. The velocity of spatial population expansion. Journal of Mathematical Biology 28:529–565.

Weinberger, H. F. 1982. Long-time behavior of a class of biological models. SIAM (Society for Industrial and Applied Mathematics) Journal of Mathematical Analysis 13:353–396.

Wright, H. E., Jr. 1992. Patterns of Holocene climatic change in the midwestern United States. Quaternary Research 38:129–134.

Wyckoff, P. H., and J. S. Clark. 2000. Predicting tree mortality from diameter growth: a comparison of maximum likelihood and Bayesian approaches. Canadian Journal of Forest Research 30:156–167.

Associate Editor: Lewi Stone